Impact of infrared radiation on oxide layer of ultrathin TiNi-based alloy wire

Gunther Sergey[1], Chekalkin Timofey[1,2]*, Hodorenko Valentina[1], Kang Ji-hoon[2], Kim Ji-soon[3], Gunther Victor[1]

[1]*Research Institute of Medical Materials, Tomsk State University, ul. 19 Gv. Divizii 17, Tomsk, 634045, Russia*
[2]*Material Research Laboratory, Kang&Park Medical Co., 48 Jungsimsangeob-2 ro, Ochang-eub, 28119, S. Korea*
[3]*School of Material Science and Engineering, University of Ulsan, 93 Daehak-ro, Ulsan, 44610, S. Korea*

*Corresponding author

DOI: 10.5185/amlett.2018.1821
www.vbripress.com/aml

Abstract

Despite the well-known advantages of TiNi-based alloys, the cost of production is still high. The alloys are traditionally made by vacuum induction melting technology followed by vacuum arc remelting to get ingots which are further worked mechanically to final or semi-finished items. The special attention is paid by a thin wire which can be used as a suture material or for a tissue grafting. Thin TiNi yarns are produced by cold drawing via dies with the intermediate annealing. When a diameter is about or over 1 mm, the existing solutions give clear insight into a general idea about how to change the structure and properties of the alloy. However, when the size is definitely scaled-down to 90 μm and less, serious difficulties appear because such yarn requires thoroughly care in mechanical processing steps and repeated heat treatment increases the expense making the product costly and unprofitable. As working steps and heat treatment of the ultrathin TiNi-based wire (UW) are to be more predictable and controllable, there was suggested an infrared (IR) drawing heater due to the radial warming system located prior to the die. In hope to provide a more comprehensive understanding of this issue, a study on how the IR heating method influences on surface properties of the UW, comparing the various effects of heat treatment was carried out using the designed IR heater. The study covers the effect of oxide layer composition and its modification on the properties of the wire IR-heat drawn. Strong correlations were observed between oxide layer thickness and strength characteristic of the resultant wire. These findings elucidate the role of the oxide layer and its composition on a quality of the UW drawing process.

Keywords: TiNi-based alloy, ultrathin wire, IR drawing, ductility, elemental analysis.

Introduction

TiNi-based alloys are widely used in clinical practice. Such alloys show unique properties which include shape memory effect, superelasticity, high corrosion resistance, strength etc [**1**]. Similar to the living tissue, TiNi-based alloys have stress-strain behavior which favorably distinguishes them from other grafting materials [**2**]. Currently, the need for the UW for numerous medical applications is constantly increasing [**3-5**]. The UW is a semi-finished product used in fabricating a surgical suture material, metallic fabric and knitted wire mesh for a grafting (general and vascular surgery, oncosurgery etc.), working elements for orthodontic devices, fixtures for the detached retina, and artificial ligaments for ruptured tendons etc. [**6-9**]. The quality of the semi-finished TiNi-based items and their properties is determined by the alloy's composition and heat/mechanical working history.

Heat treatment comprises herein both the annealing/quenching and related effects within the temperature range 450–850^{0}C [**10**]. Mechanical treatment is usually limited by working of the material within 10–15% of the strain including both a plastic- and martensite one (6–10%). It is important to understand that heat treatment of TiNi-based materials are also an essential part of alloy processing and device manufacturing. Temperatures about 700 ^{0}C are employed for wire annealing during its drawing; the temperatures within 450÷550 ^{0}C gap are used to design optimal shape memory and superelasticity, and for shape setting procedure. Heat treatments at temperatures being less 300 ^{0}C are customarily associated with the processes of surface modifications and are also sometimes employed in the fabrication of stent grafts for attaching polyester fabric [**11**]. Not only the above heat solutions may modify the phase composition of the bulk, but they also modify either Ti- or Ni-rich surface sub-layers. The coexistence of various chemical compounds such as TiNi(Me) alloys with the binary and ternary metal oxides as well as oxicarbonitrides in the surface layers may enhance Nitinol biocompatibility [**12, 13**]

One of the known problem includes the manufacturing of the UW (<90 μm) which has a

homogeneous composition and whole length similar characteristics. When the further working, i.e. a drawing, is applied, in order to fix the structure and physical-mechanical properties of the treated alloy, one needs to provide conditions both for the actual annealing to eliminate the residual stress or phase hardening and for active plastic flow. Present techniques using the furnace for the annealing of the UW are beneath criticism since they don't provide the specified heat mode because such a thermal effect on the moving wire when drawing becomes unpredictable so long as the UW gets either overheated or not heated sufficiently that leads to its failure or breaking.

Therewith, a very important factor when drawing is to take into consideration the latent heat which accompanies all the induced martensite transitions [**14**]. The thinner the UW, the faster it gets cool. The essence of IR irradiation is to increase the quality of the UW drawing owing to the thermal impact, which reduces defect's appearance and wire break as a result of advanced heat distribution allowing the fiber being hot drawn. It provides the thermal condition wherein the UW remains heated as far as the die inlet.

The manufacturing process of the UW is rather hard and costly since it consists of a sequence of working stages including a multiple hot rolling followed by swaging and drawing with intermediate heat solutions. Although published studies demonstrate the importance of applied working steps on the composition of the oxide layer and its impact on the thin wire behavior and its characteristics, the comparative performance in the suggested IR- and traditional drawing of the UW has yet to be explored.

The objective of the study is to gain an insight into the improved UW drawing method by elucidating the relationships between oxide layer thickness and its composition, and the effect IR heating on structural and strength characteristics of the resultant UW.

Experimental

The designed IR LED heater (**Fig. 1**) emits IR irradiation circularly in front of the die having an impact on the UW surface structure only. The working part of the device consists of 6 in-parallel connected cylindrical components being detached. The latter totally comprise 96 IR LEDs ("Kingbright" type L-34F3BT, wavelength – 940 nm, power – 140 mW).

UW samples were fabricated from the TN-10 brand alloy [**15**]. They were repeatedly drawn from ∅1.5 mm wire using synthetic polycrystalline diamond dies and oil-based lubricants to a finished diameter of 30 μm. To get the said UW specimens, standard reduction and heat treatment by interpass annealing at a temperature of 650 ^{0}C was used for a cold drawing down to ∅0.50 mm followed by i) the same drawing procedure when interpass annealing was performed at a temperature of 500 ^{0}C and ii) the IR heater was additionally involved for a hot drawing when the wire surface layer was IR heated at a temperature less 200 ^{0}C.

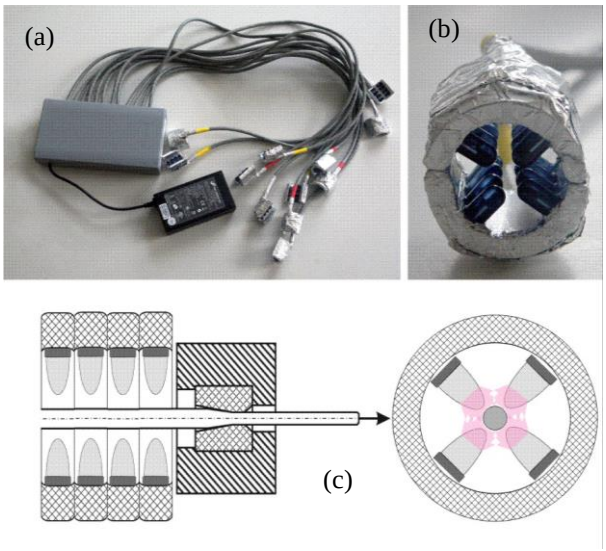

Fig. 1. Designed IR heater for the UW drawing process: (a) general view; (b) single heating component comprising 16 LEDs, (c) outline of the suggested IR drawing process when the only surface layer is heated.

All as-drawn samples for microstructural examination were prepared according to the standard metallographic specimen preparation procedure. Details about the applied procedure can be found in [**16, 17**]. Microstructural studies were made using a scanning electron microscope (SEM) by Jeol JSM 6500F, and the phase compositions were determined using energy-dispersive spectroscopy (EDS) by EDAX ECON IV. The consistency of data acquired was confirmed by numerous measurements.

Comparative microstructural assessment of oxygen content in UW as-drawn samples, 30, 60 and 80 μm in dia, obtained both using the IR irradiation and according to a conventional technology was carried out by probing each sample in two fields of the cross-section: the center proximate and the near edge encircles. Elemental concentration data were further plotted versus the UW dia.

Ultimate tensile test properties were measured using a conventional screw-driven testing machine Instron-4206 at the room temperature, and the strain rate was at 10^{-3} s^{-1}. The loading continued until the sample reached the breakpoint. The load history in terms of force-displacement was recorded and plotted as well.

Results and discussion

The main intermetallic TiNi compound of the UW bulk comprises the *B*2 parent and *B*19' martensitic phase. A large number of Ti- and Ni-rich precipitates, which are inhomogeneously distributed in the matrix, were found (**Fig. 2**). Coarse Ti2Ni precipitates are incoherent as compact spots or clusters. On contrary, fine TiNi3 precipitates are coherent having, as a rule, somewhat round or plate shape and few ones are as a grid f a smaller size.

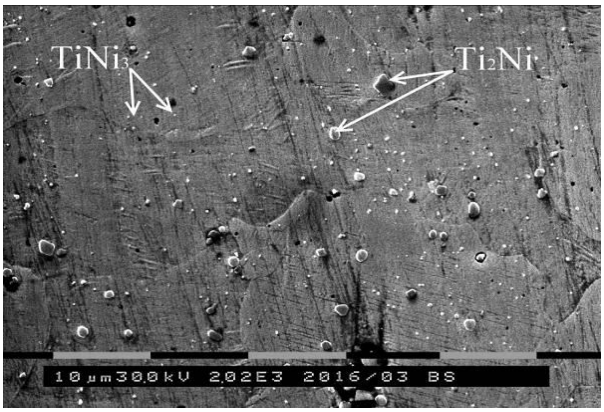

Fig. 2. SEM microstructural details of the UW cross-section.

The irregular oxide film is shown by longitudinal textured patterns (as slivers, scratches, fissures etc.) which are characterized by a cellular and flaky microporous structure **(Fig. 3)**. The rough pattern is well pronounced in ∅80 μm UW samples, while the surface morphology changes and the pattern become smoothen in reducing the diameter down to 30 μm. Such a kind of the structure is due to redundant plastic flow by passing through a series of drawing dies followed by interpass heat solutions.

EDS assessment of the UW surface showed the oxygen content decrement in the surface layer when drawing. This is due to drawing features as the material is being deformed through the die, strain hardening

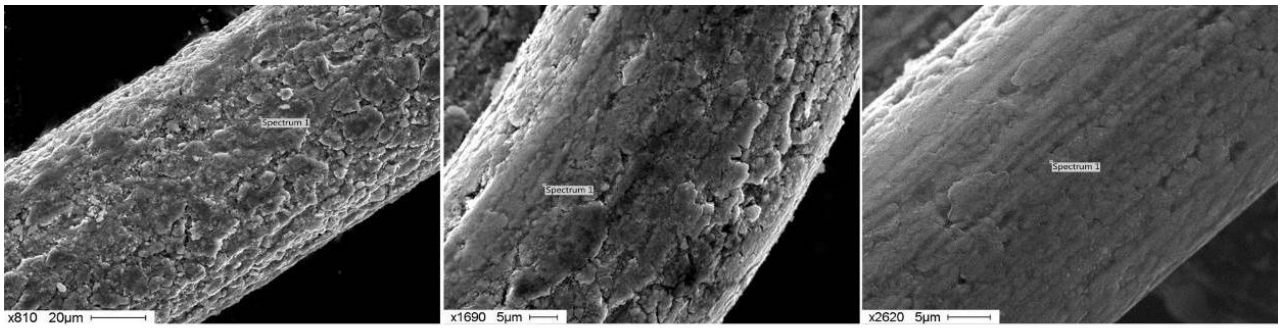

Element	wt.%	at.%
O	27.10	52.03
Ti	28.64	21.54
Ni	44.26	26.43

Element	wt.%	at.%
O	24.54	44.85
Ti	33.72	27.24
Ni	41.74	27.91

Element	wt.%	at.%
O	11.85	29.61
Ti	30.34	27.53
Ni	57.81	42.86

Fig. 3. SEM details of rough, granular, irregular, and flaky surface with lots of micropores and EDS data of the non-IR drawn UW samples: (a) 80; (b) 60; (c) 30 μm in dia.

Totally, the UW is a composite material consisting of the bulk and irregular oxide layer as shown in Fig. 1, which serves as a protective barrier against any metal ion release and facilitates the incorporation of an implant made of the UW in human tissues, since crystalline-structure oxide is more favorable to promoting the biocompatibility when compared to amorphous oxides or coatings [**18, 19**]. The said oxide layer imparting specific biocompatible properties, in particular, to TiNi-based mesh endografts [**2, 3, 5, 8**], is mainly TiO_2, which is formed by a repeated drawing with interpass annealing.

When a heat treatment is applied, Ti is known to segregate to free surfaces of TiNi whereby the oxide film is formed [**20**]. The segregation behavior to the surface and interface in the TiNi-based alloy has already been experimentally confirmed [**21, 22**]. Annealing suppresses the surface Ni content possibly due to the consolidation of titanium oxide, which has higher heats of formation compared to that of nickel oxide. As a result, Ni segregated away from the surface. The oxide layer formation is affirmed to be governed primarily by the oxidation kinetics and diffusion of Ti through the oxide [**23, 24**]. In our study, the oxide layer thickness was found to decrease nonlinearly with reducing the UW diameter, i.e. for a wire of ∅1 mm, it varies within 15÷25 μm, and for a yarn of ∅30 μm, it may vary within 2÷4 μm.

occurs and the UW is severely strain-hardened. Obviously, plastic strain in the UW drawing process, and hence, work hardening, is greater in the surface layer as compared to sub-layers. When drawing the UW of smaller diameter, the oxide film becomes thinner, and therefore, interpass annealing is performed at lower temperatures, which naturally decreases the activity of titanium for oxygen.

Comparative elemental assay of the matrix and surface layer of as-drawn UW samples fabricated by a traditional method and using the IR heater is shown in **Figs. 4-5**.

An analysis of the obtained results demonstrates that IR radiation impacts differentially on the UW depending on its diameter. As mentioned above, IR radiation has no significant effect on the UW matrix, but mainly affects the structure of the surface layer. There was no both Ti and Ni concentration change in the matrix. On contrary, the surface layer concentration, after additional exposure to IR radiation, drastically changed, especially the oxygen, therefore, both Ti and Ni content also changed.

A redistribution of Ti, Ni and O content within the surface layer depending on the diameter of UW samples drawn by the conventional technology and using the IR heater is compared in **Fig. 6** so as to clarify the difference. Obviously, when drawing, the oxygen content in all non-IR drawn samples decreases while both Ti and Ni content increases. As the UW becomes

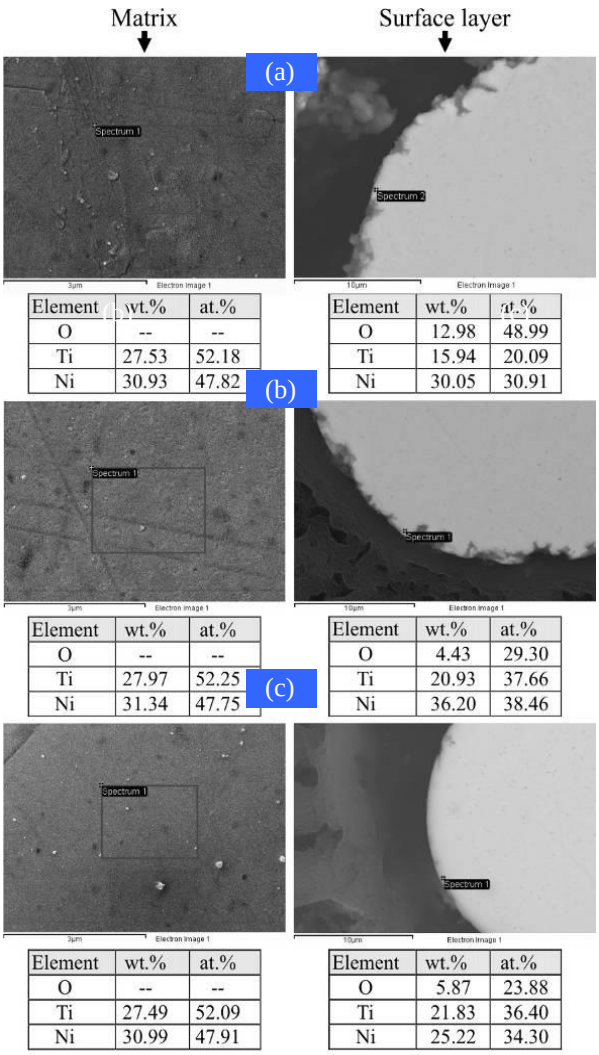

Element	wt.%	at.%
O	--	--
Ti	27.53	52.18
Ni	30.93	47.82

Element	wt.%	at.%
O	12.98	48.99
Ti	15.94	20.09
Ni	30.05	30.91

Element	wt.%	at.%
O	--	--
Ti	27.97	52.25
Ni	31.34	47.75

Element	wt.%	at.%
O	4.43	29.30
Ti	20.93	37.66
Ni	36.20	38.46

Element	wt.%	at.%
O	--	--
Ti	27.49	52.09
Ni	30.99	47.91

Element	wt.%	at.%
O	5.87	23.88
Ti	21.83	36.40
Ni	25.22	34.30

Fig. 4. SEM patterns and EDS data of the non-IR drawn UW samples: (a) 80; (b) 60; (c) 30 μm in dia.

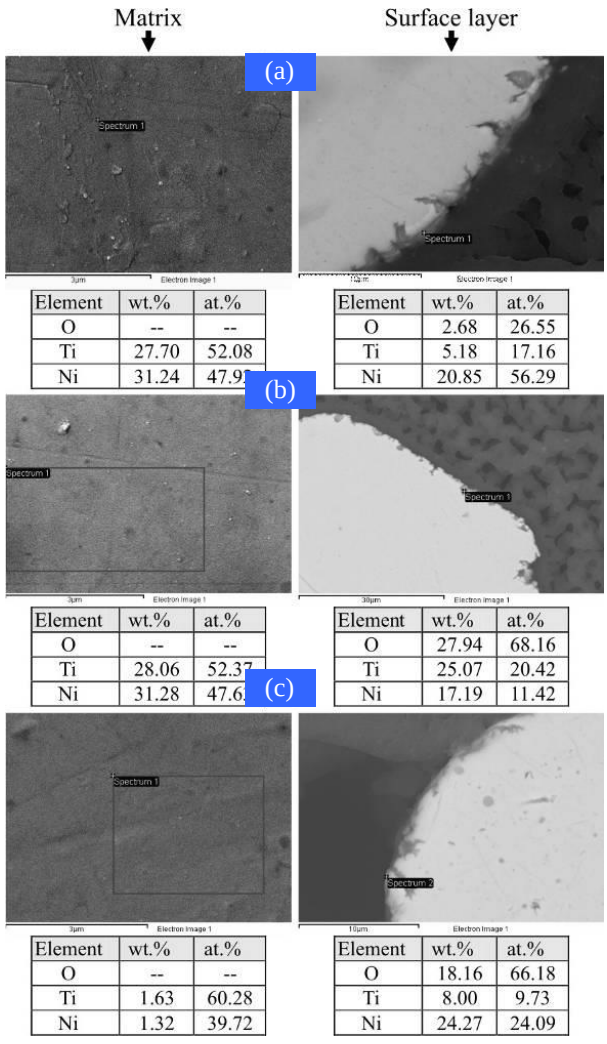

Element	wt.%	at.%
O	--	--
Ti	27.70	52.08
Ni	31.24	47.9

Element	wt.%	at.%
O	2.68	26.55
Ti	5.18	17.16
Ni	20.85	56.29

Element	wt.%	at.%
O	--	--
Ti	28.06	52.37
Ni	31.28	47.6

Element	wt.%	at.%
O	27.94	68.16
Ti	25.07	20.42
Ni	17.19	11.42

Element	wt.%	at.%
O	--	--
Ti	1.63	60.28
Ni	1.32	39.72

Element	wt.%	at.%
O	18.16	66.18
Ti	8.00	9.73
Ni	24.27	24.09

Fig. 5. SEM patterns and EDS data of the IR drawn UW samples: (a) 80; (b) 60; (c) 30 μm in dia.

thinner, the thickness of the surface layer, where the oxygen content strongly depends on the annealing time, decreases. In this case, the thinner the UW, the faster it cools before a die inlet and this process can be described as a cold drawing and, therefore, the oxygen content shows the decrement. Accordingly, the content of titanium and nickel increases.

On contrary, in the IR drawn samples, the oxygen content drastically increases as both Ti and Ni content decreases. This fact can be explained in terms of hot drawing process when the UW being favorably heated as far as a die inlet, and so the surface layer suffers the higher thermal oxidation. Moreover, the nickel content in the surface layer drops drastically compared the initial diameter.

Since the main impact of IR radiation is directed to a local heating of the oxide layer and the following bulk sublayer, it leads to a decrease in yield strength and increases ductility by stretching the UW. Other words, the IR radiation makes an excitation of atoms to a limited extent, which leads to an increased temperature of the material (local heating), and, consequently, reduces the yield strength of the alloy followed by an increase of its ductility. In this case, the response of different areas of the material to IR radiation is intricate. The TiNi bulk being undergone IR radiation, virtually, does not react but showing a little heating of the yarn.

The TiNi bulk is characterized by a high level of mechanical characteristics, its relaxation behavior gives the UW rubber-like properties and high elasticity – allowing strain on the order over 8% due to the stress induced transformation, followed by strain recovery (and concomitant phase transformation back to the parent austenite) upon removal of the applied stress [**25**, **26**]. In contrast to the behavior of the bulk, the surface layer shows low levels of ductility and increased brittleness; hence, in drawing the UW, its surface is a source of cracks, chips, and other defects. A combination of the high plasticity of the UW and a positive IR effect on the surface layer promotes the greater technological efficiency of the wire drawing. The UW quality is determined not only by properties of the ingot, but also dynamic changes during a machining. Along with the change of the workpiece geometry, substantial change of physico-mechanical characteristics of the processed alloy structure occurs.

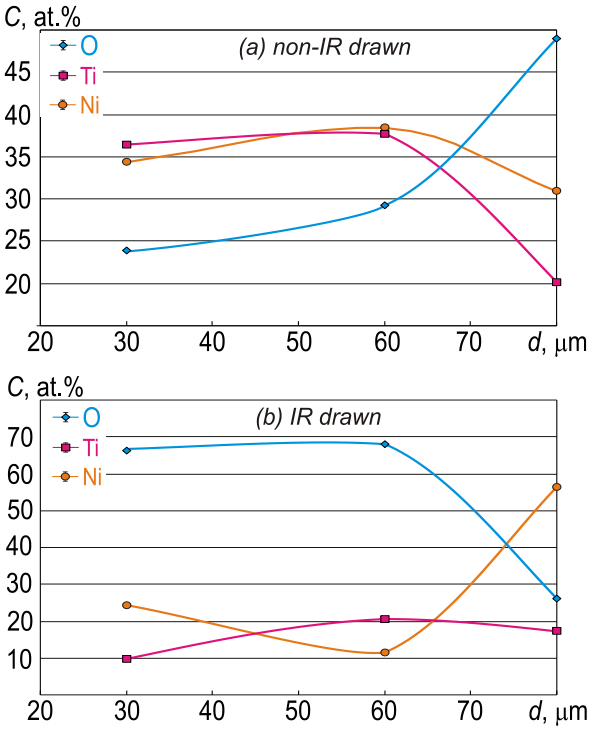

Fig. 6. Elemental (Ti, Ni and O) content within the surface layer vs the UW dia in non-IR (a) and IR (b) drawn samples.

The tensile test gives additional information for comprehensive understanding the UW nature and its stress-strain characteristics (**Fig. 7**). In reducing the UW diameter, the UTS increases and even at a dia of 30 μm and reach a value of 190 kgf/mm^2. Such the UTS increased is due to a strain hardening which occurs in the process of wire drawing. It should be noted the effect of phase hardening on the increased concentration of both Ti- and Ni-rich precipitates (Ti_2Ni, $TiNi_3$, and Ni_4Ti_3). In this case, the ratio of Ti and Ni content in the bulk varies, based on the fact that the smaller UW diameter is, the higher tensile strength observed. Other words, for the UTS it meant the thinnest UW could take more stress before a failure what is very much in line with the previous findings of other researchers [**27**]; it typically occurs in Ni-rich alloys and is also confirmed by data shown in **Fig. 6**.

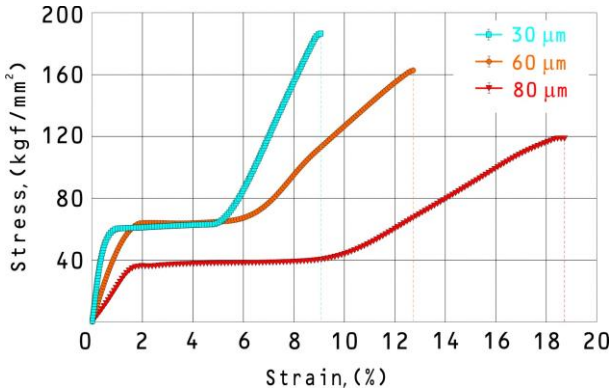

Fig. 7. Stress-strain relationship of IR drawn UW samples.

The oxide layer has a strong effect on bulk's characteristics, despite the fact that its thickness decreases when drawing, though its volume fraction in the UW grows. At the same time, this surface composite film plays a role of the sheath tightly enveloping the UW matrix, what is able to impart some increment to the UTS.

As said, the effect is caused by Ti depletion in the bulk when the martensitic points move towards the low-temperature range and, hence, ∅30 μm sample becomes more stiff at the ambient temperature. The martensite strain shows a decrement 9.5% (∅80 μm) to 5.3% (∅30 μm). Obviously, the increased volume fraction of the oxide layer makes the UW bulk exhibiting shape memory and related effects grow scanty. The contribution of plastic strain to elongation due to strain hardening also decreases from 9.0% (∅80 μm) to 3.6% (∅30 μm). The overall strain at the breakpoint goes down as well from 18.5% (∅80 μm) to 9.0% (∅30 μm), although the stress-induced martensite level varies slightly within 40÷60 kgf/mm^2.

Conclusion

Samples of ∅30 μm UW have been drawn due to the technique designed, so it allowed us to suggest a superior material for mesh medical devices. The UW is surface heated, what results in the surface layer plasticity, where the maximum strain takes place while drawing, increases remarkably. The nature of IR preheating drawing is thereby to recover a balance between the IR heating and the latent heat absorption due to the interface shear. IR heating reduces the drawing effort, meanwhile, it expands the plasticity of the worked wire as well as an ultimate tensile strength, what obviously decreases the number of UW breakage.

Comparative assessment of the IR and non-IR drawn UW has shown the elemental redistribution (Ti, Ni, and O) of the oxide layer changed drastically in reducing the UW diameter. The IR drawing technique makes O content increment more pronounced and apparent. It owes its gain to the segregation behavior both Ti and Ni during working steps.

The oxide layer plays a role of restraint jacket densely enveloping the UW and increasing its ductility since beginning from 0.06 mm and less the oxide layer is a favorable argument improving the tensile strength. It happens due to the Ni-rich phases which harden the bulk and once the dia has been reduced down to 0.03 mm, the UTS reaches about 1900 MPa.

Acknowledgements

This study was supported by Government Assignment #3.6492.2017/6.7 and #HY3.6492.2017/BY.

References

1. Gunther, V.E.; Hodorenko, V.N.; Chekalkin, T.L. et al.; Medical materials and shape memory implants: In 14 vol. / Shape memory medical materials, Tomsk: MIC, **2011**, 1. **ISBN**: 9785985890440

2. Muhamedov, M.; Kulbakin, D.; Gunther, V. et al.; *J. Surg Oncol*., **2015**, *111*, 231.
DOI: 10.1002/jso.23779
3. Kulbakin, D.; Chekalkin, T.; Muhamedov, M. et al.; *Case Rep. Oncol*., **2016**, *9*, 772.
DOI: 10.1159/000452790
4. Kokorev, O.; Hodorenko, V.; Chekalkin T. et al.; *Artif. Cells Nanomed. Biotechnol*., **2016**, *44*,704.
DOI: 10.3109/21691401.2014.982799
5. Zilla, P.; Moodley, L.; Wolf, M. et al.; *J. Vasc. Surg.*, **2011**, *54*, 1439.
DOI: 10.1016/j.jvs.2011.05.023
6. Lanshakov, V.A.; Gunther, V.E.; Plotkin, G.L. T.L. et al.; Medical materials and shape memory implants: In 14 vol. / Shape memory medical materials, Tomsk: MIC, **2010**, 2.
ISBN: 9785985890426
7. Zapuskalov, I.V.; Gunther, V.E.; Stebluk, A.N. et al.; Medical materials and shape memory implants: In 14 vol. / Shape memory medical materials, Tomsk: MIC, **2012**, 14.
ISBN: 9785985890495
8. Schoettler, J.; Jussli-Melchers, J.; Grothusen, C. et al.; *Interact. Cardiovasc. Thorac. Surg.* **2011**, *13*, 396.
DOI: 10.1510/icvts.2010.265116
9. Singh, C.; Wang, X.; *J. Mech. Behav. Biomed. Mater.*, **2015**, *48*: 125.
DOI: 10.1016/j.jmbbm.2015.04.001
10. Xu, L.; Wang, R.; *Mod. Appl. Sci.*, **2010**, *4*: 109.
DOI: 10.5539/mas.v4n12p109
11. Shabalovskaya, S.; Anderegg, J.; Van Humbeeck, J.; *Acta Biomater*., **2008**, *4*: 447.
DOI: 10.1016/j.actbio.2008.01.013
12. Sullivan, S.J.; Dreher, M.L.; Zheng, J. et al.; *Shap. Mem. Superelasticity*, **2015**, *1*, 319.
DOI: 10.1007/s40830-015-0028-x
13. Anikeev, S.; Hodorenko, V.; Chekalkin, T. et al.; *Smart Mater. Struct.*, **2017**, 26, 057001.
DOI: 10.1088/1361-665X/aa681a
14. Gunther, V.E.; Chekalkin, T.L.; Kim , J.S. et al.; *Adv Mater Lett.*, **2015**, *6*, 8.
DOI: 10.5185/amlett.2015.5597
15. Gunther, V.E.; Dambaev, G.Ts.; Sysolyatin, P.G. et al. Delay law and new class of materials and implants in medicine, Northampton, MAA: STT, **2000**.
ISBN: 0970235305
16. Bramfitt, B.L.; Benscoter, A.O.; Metallographer's Guide: Practices and Procedures for Irons and Steel; ASTM International: Ohio, **2012**.
DOI: 10.1361/mgpp2002p169
17. *ASTM Standard F3122-14*.; ASTM International, West Conshohocken, **2014**.
DOI: 10.1520/F3122-14
18. Munroe, N.; Pulletikurthi, C.; Haider, W.J.; *Mater Eng Perform.*, **2009**, *18*, 765.
DOI: 10.1007/s11665-009-9454-2
19. Li, C.Y.; Yang X.J.; Zhang L.Y. et al.; *Mater. Sci. Eng. C*, **2007**, *27*, 122.
DOI: 10.1016/j.msec.2006.03.004
20. Hansena, A.W.; Beltramia, L.V.; Antoniniet L.M. et al.; *Mat. Res.*, **2015**, *18*, 1053.
DOI: 10.1590/1516-1439.022415
21. Yeung, K.W.; Poon, R.W.; Chu, P.K. et al.; *J. Biomed. Mater. Res.*, **2007**, *82A*, 403.
DOI: 10.1002/jbm.a.31154
22. Freiberg, K.E.; Bremer-Streck, S.; Kiehntopf, M. et al.; *Acta Biomater*., **2014**, *10*: 2290.
DOI: 10.1016/j.actbio.2014.01.003
23. Undisz, A.; Hanke, R.; Freiberg, K.E. et al.; *Acta Biomater.*, **2014**, *10*: 4919.
DOI: 10.1016/j.actbio.2014.07.018
24. Xu, C.H.; Ma, X.Q.; Shi, S.Q. et al.; *Mater. Sci. Eng. A*, **2004**, *371*, 45.
DOI: 10.1016/S0921-5093(03)00287-9
25. Robertson, S.W.; Pelton, A.R.; Ritchie, R.O.; *Int. Mater. Rev.*, **2012**, *57*, 1.
DOI: 10.1016/S0921-5093(03)00287-9
26. Jani, J.M.; Leary, M.; Subic, A. et al.; *Mater. Design*, **2014**, *56*, 1078.
DOI: 10.1016/j.matdes.2013.11.084
27. Norwich, D.W; Fasching, A.J.; *Mater. Eng. Perform.*, **2009**. *18*, 558.
DOI: 10.1016/j.matdes.2013.11.084

